

Three-Dimensional Finite Element Superconvergent Gradient Recovery on Par6 Patterns

Jie Chen and Desheng Wang*

Division of Mathematical Sciences, School of Physical and Mathematical Sciences, Nanyang Technological University, 21 Nanyang Link, Singapore 637371.

Received 15 September 2009; Accepted (in revised version) 6 January 2010

Available online 8 March 2010

Abstract. In this paper, we present a theoretical analysis for linear finite element superconvergent gradient recovery on Par6 mesh, the dual of which is centroidal Voronoi tessellations with the lowest energy per unit volume and is the congruent cell predicted by the three-dimensional Gersho's conjecture. We show that the linear finite element solution u_h and the linear interpolation u_l have superclose gradient on Par6 meshes. Consequently, the gradient recovered from the finite element solution by using the superconvergence patch recovery method is superconvergent to ∇u . A numerical example is presented to verify the theoretical result.

AMS subject classifications: 65N30

Key words: Superconvergence, Par6, finite element method, centroidal Voronoi tessellations, Gersho's conjecture.

1. Introduction

Superconvergence of the gradient for the finite element approximation is a phenomenon whereby the convergent order of the derivatives of the finite element solutions exceeds the optimal global rate. Extensive research works have been done on this active research topic (see, e.g., Wahlbin [1], Křížek [2], Chen and Huang [3]). Various postprocessing techniques are raised to recover the gradients with high order accuracy from the finite element solution, such as the well-known Superconvergence Patch Recovery (SPR) method introduced by Zienkiewicz and Zhu [4] and Polynomial Patch Recovery (PPR) method raised by Zhang and Naga [5]. The superconvergence property in the gradient recovery has been applied to a posterior error estimation and mesh adaptivity with huge success, especially in numerical simulations in engineering [6–10].

The geometric structure of the computational mesh has great influence on the superconvergence property. It is well-known that superconvergence property is preserved for

*Corresponding author. *Email addresses:* chen0437@ntu.edu.sg (J. Chen), desheng@ntu.edu.sg (D. Wang)

both the function values of finite element solution and its derivatives on equilateral meshes. However the requirement of an equilateral mesh is too stringent and usually it is impossible to generate such a mesh for a general domain, even for a simple rectangular domain. Thus some geometric conditions are imposed on computational meshes to guarantee the superconvergence property, such as the $\mathcal{O}(h^2)$ approximate parallelogram property by Xu and Bank [11, 12]. But questions such as what kind of meshes satisfy these conditions and how to generate these meshes are still unsolved. Recently, these questions are partially answered in [13, 14]. The superconvergence based on centroidal Voronoi tessellation (CVT) for linear finite element approximation is reported and based on this result a posterior error estimator and corresponding adaptive CVT-based mesh generation method are also raised. This finding is extended to three dimension by Chen, Huang and Wang [15] with a new recovery method: Modified Superconvergence Patch recovery (MSPR) method to overcome the influence of slivers. The theoretical proof for superconvergence property based on general CVT meshes seems quite difficult.

We take the initial step by giving the theoretical analysis of superconvergence property on a particular CVT structure: Par6 tessellation. The details of Par6 are presented in Section 2. Following earlier works [16, 17], we first present the result that the gradient of the linear finite element approximation u_h is superconvergent to the gradient of the piecewise linear interpolant u_I of the solution u . More precisely, we have

$$\|u_h - u_I\|_{1,\Omega} \lesssim h^2 \|u\|_{3,\infty,\Omega}.$$

Here the convergence order is approximately $\frac{1}{2}$ higher than general cases on general CVT meshes because of the highly symmetric structure of Par6 tessellation. The low order terms in the asymptotic expansion of the local error are totally canceled on Par6 structure. The errors on the boundary are also treated in this estimation. The second major part of this proof is that the gradient recovered by SPR is superconvergent to true gradient, that is to say

$$\|\nabla u - G_h u_h\|_{0,\Omega} \lesssim h^2 \|u\|_{3,\infty,\Omega},$$

where G_h is the SPR recovery operator. Both the superconvergence and the gradient recovery results are for a non-self-adjoint and possibly indefinite problem.

The rest of this paper is organized as follows. A detailed introduction of Par6 tessellation is given in Section 2. The theoretical proof of superconvergence property on Par6 tessellation is presented in Section 3. And in Section 4, numerical example is presented to verify the theoretical result. Finally, some conclusions are drawn in Section 5.

2. Par6 pattern: the optimal centroidal Voronoi tessellation in three dimensional space

Par6 pattern is a assembly which can be repeated indefinitely to fill space [18]. Different from two dimensional case, regular tetrahedrons, unlike equilateral triangles, can not be fitted together to fill space. Par6 assembly is obtained by distorting a cube into a

parallelepiped involving a 35.3° rotation of the edges about the y - and z -axis. And then each parallelepiped is divided into six identical tetrahedrons. Furthermore, the four faces of these tetrahedrons are all the same—an isosceles triangle with one edge of length p and the other two of length $\sqrt{3}p/2$. Repeating this assembly to get Par6 tessellation (see Fig. 1).

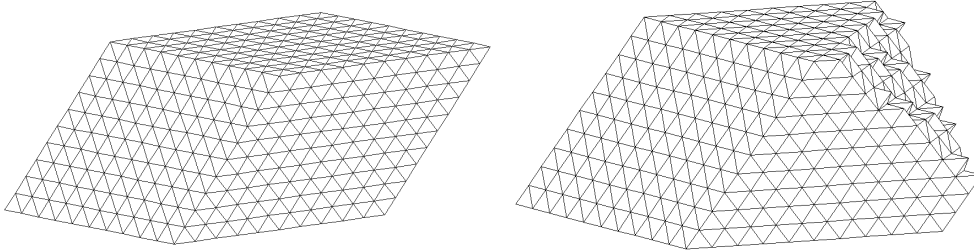


Figure 1: Par6 tessellation.

Par6 based centroidal Voronoi Tessellation has the lowest energy per unit volume and is the most likely congruent cell predicted by the three-dimensional Gershó's conjecture [19]. Given a density function ρ , a tessellation $V = \{V_i\}_1^n$ of the domain Ω and a set of points $Z = \{z_i\}_1^n$ in Ω , we can define the following cost functional:

$$\mathcal{F}(V, Z) = \sum_{i=1}^n F(V_i, z_i), \quad \text{where } F(V_i, z_i) = \int_{V_i} \rho(x) \|x - z_i\|^2 dx.$$

The energy per unit volume (E_p) for a partition or tessellation $\{V, Z\}$ is then defined by:

$$D(V, Z) = \frac{n^{2/k} \mathcal{F}(V, Z)}{k |\Omega|^{1+2/k}}.$$

Here, k is the dimension of the space ($k = 3$ in this paper), $|\Omega|$ the volume of $\Omega = \bigcup_{i=1}^n V_i$.

For a given bounded domain Ω together with a specified density function and a fixed number of generator, an *optimal CVT* is defined as a global minimum of $\mathcal{F}(V, Z)$, while the optimal centroidal Voronoi tessellation in a given Euclidean-dimensional space (e.g., the two-dimensional space), asymptotically speaking, is defined as the CVT which has the lowest energy per unit volume among all CVTs that cover the whole space (as the number of generators going to infinity).

The optimal CVT concept is closely related to the Gershó's conjecture [20], which states that: *asymptotically speaking, all cells of the optimal CVT, while forming a tessellation, are congruent to a basic cell which depends on the dimension.* This claim is trivially true in one dimension. It has been proved for the two-dimensional case [21] with the basic cell being the two-dimensional regular hexagon. Gershó's conjecture remains open for three and higher dimensions [22]. In [23], it was shown that the body-centered-cubic (BCC, see Fig. 2) lattice based CVT enjoys the lowest energy per unit volume among all possible

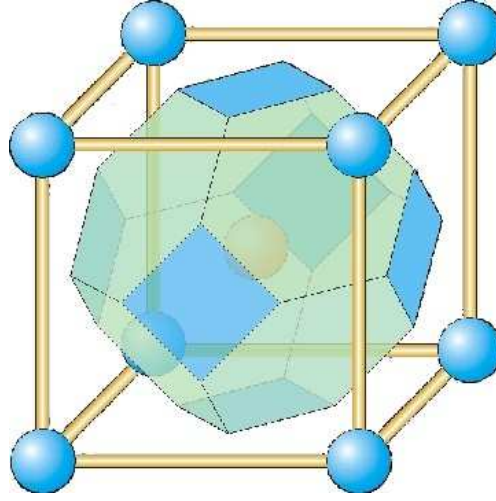


Figure 2: Basic Voronoi cell of BCC configuration.

lattice based CVTs. The BCC based CVTs has the energy per unit volume valued at 0.07854, with the basic cell given by the truncated octahedron.

For nonlattice based or general CVTs, it remains unresolved whether the BCC enjoys the lowest energy per unit volume [22]. One question pertains to the possibility of having the optimal CVT made up by a combination of several types of basic cells. In [19], a series of numerical examples are designed for both lattice and nonlattice based CVTs. The computed energy per unit volume and other related properties and statistics substantiate the claim of the three-dimensional Gershgorin's conjecture: *the BCC based CVT enjoys the lowest energy among all three-dimensional CVTs including both lattice and nonlattice CVTs*. Thus, asymptotically speaking, the congruent cell of the optimal CVT is the Voronoi cell of the BCC based tessellation, that is, the truncated octahedron.

3. Superconvergence on Par6

3.1. Preliminaries

The non-self-adjoint and possibly indefinite problem is considered: find $u \in H^1(\Omega)$ such that

$$B(u, v) = \int_{\Omega} (\mathcal{D}\nabla u + \mathbf{b}u) \cdot \nabla v + cuv \, dx = f(v) \quad (3.1)$$

for all $v \in H^1(\Omega)$. Here \mathcal{D} is a 3×3 symmetric positive definite matrix, \mathbf{b} a vector, and c a scalar, and $f(\cdot)$ is a linear functional. We assume that all the coefficient functions are smooth.

In order to insure that (3.1) has a unique solution, we assume that the eigenvalues of \mathcal{D} satisfy $0 < \mu < \lambda_{\min} < \lambda_{\max} < \nu$ uniformly in Ω . Let $\mathcal{V}_h \subset H^1(\Omega)$ be the space of

continuous piecewise linear polynomials associated with a quasi-uniform triangulation \mathcal{T}_h , and consider the approximate problem: find $u_h \in \mathcal{V}_h$ such that

$$B(u_h, v_h) = f(v_h) \quad (3.2)$$

for all $v_h \in \mathcal{V}_h$. The following result is standard in FEM

$$\|u - u_h\|_{1,\Omega} \leq \frac{\nu}{\mu} \inf_{v_h \in \mathcal{V}_h} \|u - v_h\|_{1,\Omega}.$$

We define the piecewise constant matrix function \mathcal{D}_τ in terms of the diffusion matrix D as follows:

$$\mathcal{D}_{\tau ij} = \frac{1}{|\tau|} \int_{\tau} \mathcal{D}_{ij} dx.$$

Note that \mathcal{D}_τ is symmetric and positive definite.

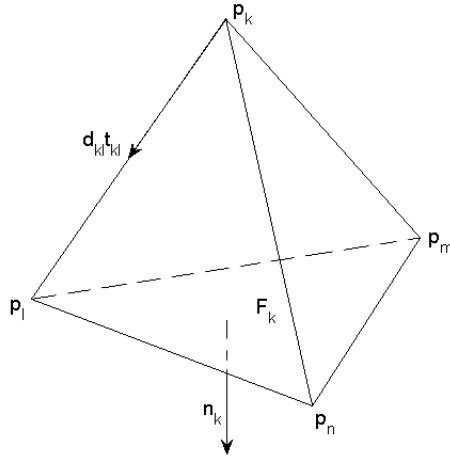


Figure 3: A tetrahedron.

Following the discussion in [17], we consider the unique shape tetrahedron τ in Par6 illustrated in Fig. 3. Let $\{\mathbf{p}_k\}_{k=1}^4$ denote four vertices of τ and the corresponding four barycentric coordinates are denoted as $\{\varphi_k\}_{k=1}^4$. We assume τ follows the orientation given by the right-hand rule and Δ_{klm} is used to denote the face with vertices $\mathbf{p}_k, \mathbf{p}_l$ and \mathbf{p}_m . If the orientation of Δ_{klm} , given by the order k, l, m , coincides with the induced orientation from τ , we say Δ_{klm} has the consistent orientation with τ . F_k is the surface opposite vertex \mathbf{p}_k with the outer normal vector \mathbf{n}_k . Let e_{ij} denote the oriented edges of element τ from \mathbf{p}_i to \mathbf{p}_j and \mathbf{t}_{ij}, d_{ij} the corresponding unit tangent vectors and edge length, respectively. Let θ_{kl} be the angle between \mathbf{t}_{kl} and the supporting plane of F_l . In general, $\theta_{kl} \neq \theta_{lk}$. Let \mathcal{D}_τ be a constant symmetric 3×3 matrix defined on τ . We define $\xi_{ij} = \mathbf{n}_i \cdot \mathcal{D}_\tau \mathbf{n}_j$. Since \mathcal{D}_τ is symmetric, $\xi_{ij} = \xi_{ji}$.

The following fundamental identity is proved in [17] for $v_h \in P_1(\tau)$ and $\phi \in H^3(\tau)$:

$$\begin{aligned} & \int_{\tau} \nabla(\phi_I - \phi) \cdot \mathcal{D}_{\tau} \nabla v_h \\ &= \sum_{k,l=1,k \neq l}^4 \frac{\partial v_h}{\partial \mathbf{t}_{kl}} \frac{\xi_{kl}}{4 \cos \theta_{kl}} \left[(d_{lm}^2 - d_{km}^2) \int_{F_k} \varphi_l \varphi_m \frac{\partial^2 \phi}{\partial \mathbf{t}_{kl}^2} \right. \\ & \quad \left. + 4 |\Delta_{klm}| \int_{F_k} \varphi_l \varphi_m \frac{\partial^2 \phi}{\partial \mathbf{t}_{kl} \partial \mathbf{n}_{kl,m}} \right] + \mathcal{O}(h^3) \|\phi\|_{3,\tau} \|v\|_{1,\tau}, \end{aligned} \quad (3.3)$$

where ϕ_I is the piecewise linear interpolant for ϕ , m is chosen such that Δ_{klm} has the consistent orientation with τ , and $\mathbf{n}_{kl,m}$ is the unit outward normal vector of edge \mathbf{t}_{kl} on the supporting plane of triangle Δ_{klm} .

3.2. Superconvergence between the FE solution and linear interpolant

A superconvergence result between the linear finite element approximation of a model second order elliptic equation and its linear interpolant is given in this section.

Recalling the property of Par6 triangulation \mathcal{T}_h . The Par6 assembly is obtained by distorting the cube into a parallelepiped with a 35.3° rotation of the edges about the y - and z -axis. Each parallelepiped is divided into six tetrahedrons and all the tetrahedrons in Par6 are the same. Furthermore, the four faces of these tetrahedrons are all the same—an isosceles triangle with one edge of length p and the other two of length $\sqrt{3}p/2 \doteq 0.866p$ (see Fig. 4).

Definition 3.1. Let \mathcal{T}_h denote the Par6 triangulation and $\mathcal{E} = \mathcal{E}_1 \oplus \mathcal{E}_2$ denote the set of edges in \mathcal{T}_h , where \mathcal{E}_1 is the set of interior edges and \mathcal{E}_2 is set of edges on the boundary. Let Ω_e denote the patch of e , which is the union of tetrahedrons sharing e .

The following lemma is the key in this paper.

Lemma 3.1. Let the triangulation \mathcal{T}_h be Par6. Let \mathcal{D}_{τ} be a piecewise constant matrix function defined on \mathcal{T}_h , whose elements $\mathcal{D}_{\tau ij}$ satisfy

$$|\mathcal{D}_{\tau ij}| \lesssim 1, \quad |\mathcal{D}_{\tau ij} - \mathcal{D}_{\tau' ij}| \lesssim h,$$

for $i, j = 1, 2, 3$. Here τ and τ' are tetrahedrons sharing a common edge. Then

$$\left| \sum_{\tau \in \mathcal{T}_h} \int_{\tau} \nabla(u - u_I) \cdot \mathcal{D}_{\tau} \nabla v_h \right| \lesssim h^2 \|u\|_{3,\infty,\Omega} |v|_{1,\Omega}. \quad (3.4)$$

Proof. Denote, with respect to τ ,

$$\alpha_{klm} = \frac{\xi_{kl}}{4 \cos \theta_{kl}} (d_{km}^2 - d_{lm}^2), \quad \beta_{klm} = \frac{\xi_{kl}}{\cos \theta_{kl}} |\Delta_{klm}|.$$

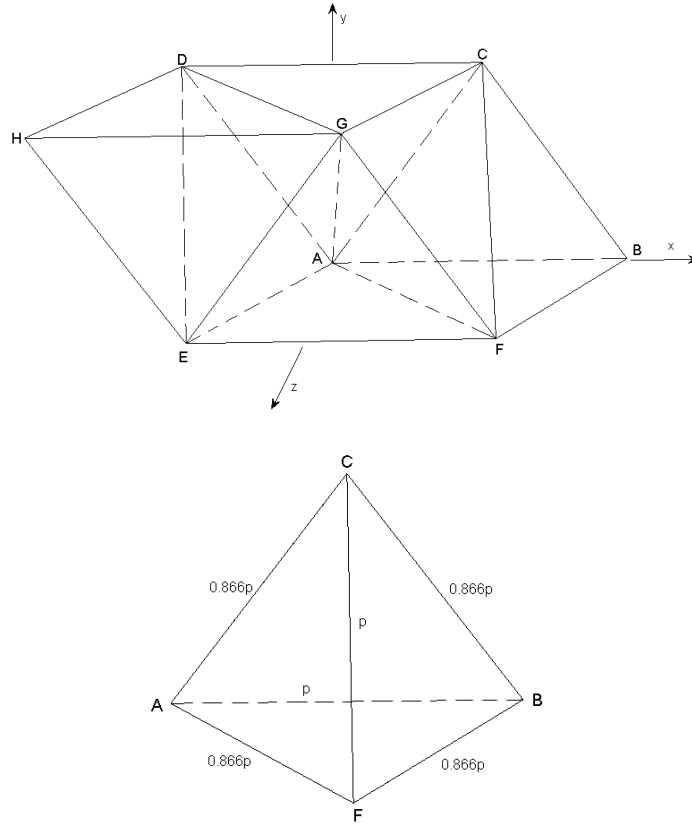


Figure 4: The Par6 assembly and the tetrahedron in Par6

Applying identity (3.3),

$$\begin{aligned} & \sum_{\tau \in \mathcal{T}_h} \int_{\tau} \nabla(u - u_I) \cdot \mathcal{D}_{\tau} \nabla v_h \\ &= \sum_{\tau \in \mathcal{T}_h} \sum_{k,l=1,k \neq l}^4 \frac{\partial v_h}{\partial \mathbf{t}_{kl}} \left[\alpha_{klm} \int_{F_k} \varphi_l \varphi_m \frac{\partial^2 u}{\partial \mathbf{t}_{kl}^2} + \beta_{klm} \int_{F_k} \varphi_l \varphi_m \frac{\partial^2 u}{\partial \mathbf{t}_{kl} \partial \mathbf{n}_{kl,m}} \right] \\ &= I_1 + I_2, \end{aligned}$$

where

$$I_i = \sum_{e_{kl} \in \mathcal{E}_i} \sum_{\tau \in \Omega_{e_{kl}}} \frac{\partial v_h}{\partial \mathbf{t}_{kl}} \left[\alpha_{klm} \int_{F_k} \varphi_l \varphi_m \frac{\partial^2 u}{\partial \mathbf{t}_{kl}^2} + \beta_{klm} \int_{F_k} \varphi_l \varphi_m \frac{\partial^2 u}{\partial \mathbf{t}_{kl} \partial \mathbf{n}_{kl,m}} \right],$$

for $i = 1, 2$. In the above formulas, F_k, α_{klm} and β_{klm} are different for different tetrahedrons. The index τ is omitted for the simplification of notation.

As mentioned before, the tetrahedrons contained in Par6 tessellation are all the same and only two types of edges are contained in Par6: edge of length p and edge of length $\sqrt{3}/2p$. From further observation on Par6 assembly shown in Fig. 4, it can be found that for interior edges, the edge of length p such as e_{AG} is shared by 4 tetrahedrons while the edge of length $\sqrt{3}/2p$, for example e_{AF} , is shared by 6 tetrahedrons. Thus we estimate I_1 in the following way.

For the edge of length p , taking e_{AG} for example, we will pair the tetrahedrons in patch $\Omega_{e_{AG}}$ one to one to cancel the low order terms. In tetrahedron τ_{AEFG} , we have term

$$\frac{\partial v_h}{\partial \mathbf{t}_{AG}} \left[\alpha_{AGE} \int_{F_{EFG}} \varphi_G \varphi_E \frac{\partial^2 u}{\partial \mathbf{t}_{AG}^2} + \beta_{AGE} \int_{F_{EFG}} \varphi_G \varphi_E \frac{\partial^2 u}{\partial \mathbf{t}_{AG} \partial \mathbf{n}_{AG,E}} \right],$$

while in tetrahedron τ_{GCDA} we have

$$\frac{\partial v_h}{\partial \mathbf{t}_{GA}} \left[\alpha_{GAC} \int_{F_{CDA}} \varphi_A \varphi_C \frac{\partial^2 u}{\partial \mathbf{t}_{GA}^2} + \beta_{GAC} \int_{F_{CDA}} \varphi_A \varphi_C \frac{\partial^2 u}{\partial \mathbf{t}_{GA} \partial \mathbf{n}_{GA,C}} \right].$$

Noticing Δ_{AGE} and Δ_{GAC} are on the same plane, we get $\mathbf{n}_{AG,E} = -\mathbf{n}_{GA,C}$. And since not only the tetrahedrons in Par6 are the same, but also the four faces of these tetrahedrons are all the same, the following identities hold:

$$\begin{aligned} \int_{F_{EFG}} \varphi_G \varphi_E \frac{\partial^2 u}{\partial \mathbf{t}_{AG}^2} &= \int_{F_{CDA}} \varphi_A \varphi_C \frac{\partial^2 u}{\partial \mathbf{t}_{GA}^2}, \\ \int_{F_{EFG}} \varphi_G \varphi_E \frac{\partial^2 u}{\partial \mathbf{t}_{AG} \partial \mathbf{n}_{AG,E}} &= \int_{F_{CDA}} \varphi_A \varphi_C \frac{\partial^2 u}{\partial \mathbf{t}_{GA} \partial \mathbf{n}_{GA,C}}. \end{aligned}$$

Using the elementary identity

$$\left| \int_F f \right| \lesssim h^{-1} \int_\tau |f| + \int_\tau |\nabla f|,$$

we get (for $\mathbf{z} = \mathbf{t}_{AG}$ and $\mathbf{z} = \mathbf{n}_{AG,E}$)

$$\int_{F_{EFG}} \varphi_G \varphi_E \frac{\partial^2 u}{\partial \mathbf{t}_{AG} \partial \mathbf{z}} \frac{\partial v_h}{\partial \mathbf{t}_{AG}} \lesssim h^{-1} \int_\tau |\nabla^2 u| |\nabla v_h| + \int_\tau |\nabla^3 u| |\nabla v_h|. \quad (3.5)$$

Coefficients α and β are estimated by

$$\begin{aligned} |\alpha_{AGE} - \alpha_{GAC}| &= 0, \\ |\beta_{AGE} - \beta_{GAC}| &= \left| \frac{\xi_{AG}}{\cos \theta_{AG}} |\Delta_{AGE}| - \frac{\xi_{GA}}{\cos \theta_{GA}} |\Delta_{GAC}| \right| \\ &= \left| \frac{|\Delta_{AGE}|}{\cos \theta_{AG}} \right| |\xi_{AG} - \xi_{GA}| \lesssim h^3, \end{aligned} \quad (3.6)$$

where $|\mathcal{D}_{\tau_{ij}} - \mathcal{D}_{\tau'_{ij}}| \lesssim h$ has been used. The other pair of tetrahedrons contained in patch $\Omega_{e_{AG}}$, say τ_{ADEC} and τ_{GCFA} , are treated in the same way.

For the edge of length $\sqrt{3}/2p$, such as e_{AF} , we also pair the tetrahedrons in patch $\Omega_{e_{AF}}$ to cancel low order terms. The only difference is that there are 3 pairs to treat in this type of patch.

Table 1: Number of tetrahedrons contained in the boundary edge patch.

Edge type	Edges on the boundary surface	Edges on the corner
length p	2	1
length $\sqrt{3}/2p$	3	depends on position

Thus combining (3.5) with (3.6) and noticing $v_h \in P_1(\tau)$, we estimate I_1 by

$$|I_1| \lesssim h^2 \int_{\Omega} (|\nabla^2 u| + h|\nabla^3 u|) |\nabla v_h| \lesssim h^2 \|u\|_{3,\Omega} |v_h|_{1,\Omega}. \quad (3.7)$$

Now we turn to the estimate for I_2 . If $v_h = 0$ on $\partial\Omega$, then it is easy to see $I_2 = 0$. For the edges on the boundary, say $e \in \mathcal{E}_2$, after carefully observation on Par6 tessellation we show the number of tetrahedrons contained in the patch Ω_e in Table 1. For the corner edges of length $\sqrt{3}/2p$, the number of tetrahedrons contained in patch Ω_e depends on the position. Corner edges that appear on position AE and CG are shared by 2 tetrahedrons, while DH and BF are only contained by 1 tetrahedron. We can pair the tetrahedrons in boundary edge patch and treat it same as before. The remaining question is how to estimate the term that can not find a partner. In general case, we define

$$B_{e_{kl}}(u) = \alpha_{klm} \frac{\partial^2 u}{\partial \mathbf{t}_{kl}^2} + \beta_{klm} \frac{\partial^2 u}{\partial \mathbf{t}_{kl} \partial \mathbf{n}_{kl,m}},$$

$$\overline{B}_{e_{kl}}(u) = |e_{kl}|^{-1} \int_{e_{kl}} B_{e_{kl}}(u).$$

Thus

$$I_2 = \sum_{e_{kl} \in \mathcal{E}_2} \sum_{\tau \in \Omega_{e_{kl}}} \int_{F_k} \varphi_l \varphi_m B_{e_{kl}}(u) \frac{\partial v_h}{\partial \mathbf{t}_{kl}}.$$

Since only the terms that can not find a partner are considered, we just need to estimate

$$\begin{aligned} \tilde{I}_2 &= \sum_{e_{kl} \in \partial\Omega} \int_{F_k} \varphi_l \varphi_m B_{e_{kl}}(u) \frac{\partial v_h}{\partial \mathbf{t}_{kl}} \\ &= \sum_{e_{kl} \in \partial\Omega} \int_{F_k} \varphi_l \varphi_m \overline{B}_{e_{kl}}(u) \frac{\partial v_h}{\partial \mathbf{t}_{kl}} - \sum_{e_{kl} \in \partial\Omega} \int_{F_k} \varphi_l \varphi_m (B_{e_{kl}}(u) - \overline{B}_{e_{kl}}(u)) \frac{\partial v_h}{\partial \mathbf{t}_{kl}}. \end{aligned}$$

For the second term, we have

$$\begin{aligned} & \left| \sum_{e_{kl} \in \partial\Omega} \int_{F_k} \varphi_l \varphi_m (B_{e_{kl}}(u) - \overline{B_{e_{kl}}}(u)) \frac{\partial v_h}{\partial \mathbf{t}_{kl}} \right| \\ & \lesssim h^3 |u|_{3,\infty,\Omega} \sum_{e_{kl} \in \partial\Omega} \int_{F_k} \left| \frac{\partial v_h}{\partial \mathbf{t}_{kl}} \right| \lesssim h^{5/2} |u|_{3,\infty,\Omega} |v_h|_{1,\Omega}, \end{aligned} \quad (3.8)$$

where the trace inequality has been used.

We now estimate the first term. Let \mathcal{P} to be the set of vertices on $\partial\Omega$. Then we have

$$\begin{aligned} & \sum_{e_{kl} \in \partial\Omega} \int_{F_k} \varphi_l \varphi_m \overline{B_{e_{kl}}}(u) \frac{\partial v_h}{\partial \mathbf{t}_{kl}} \\ & = \sum_{e_{kl} \in \partial\Omega} \overline{B_{e_{kl}}}(u) \frac{\partial v_h}{\partial \mathbf{t}_{kl}} \int_{F_k} \varphi_l \varphi_m = \sum_{e_{kl} \in \partial\Omega} \overline{B_{e_{kl}}}(u) \frac{\partial v_h}{\partial \mathbf{t}_{kl}} \frac{|F_k|}{12} \\ & = \frac{1}{12} \sum_{x \in \mathcal{P}} \left(\overline{B_{e_{kl}}}(u) - \overline{B_{e'_{kl}}}(u) \right) v_h(x) \frac{|F_k|}{|e_{kl}|}, \end{aligned}$$

where e'_{kl} is a boundary edge of a neighboring tetrahedron τ' .

It is easy to see

$$\frac{|F_k|}{|e_{kl}|} \lesssim h, \quad \left| \overline{B_{e_{kl}}}(u) - \overline{B_{e'_{kl}}}(u) \right| \lesssim h^2 |u|_{2,\infty,\Omega}.$$

Thus we get

$$\begin{aligned} & \left| \sum_{x \in \mathcal{P}} \left(\overline{B_{e_{kl}}}(u) - \overline{B_{e'_{kl}}}(u) \right) v_h(x) \frac{|F_k|}{|e_{kl}|} \right| \\ & \lesssim h^3 |u|_{2,\infty,\Omega} \|v_h\|_{\infty,\partial\Omega} \lesssim h^3 |\log h|^{1/2} |u|_{2,\infty,\Omega} \|v_h\|_{1,\Omega}, \end{aligned}$$

where the following Sobolev inequality has been used,

$$\|v_h\|_{\infty,\Omega} \lesssim |\log h|^{1/2} \|v_h\|_{1,\Omega}.$$

Following a standard argument, here $\|v_h\|_{1,\Omega}$ can be replaced by $|v_h|_{1,\Omega}$. Combining this estimate with (3.8), we have

$$\begin{aligned} |\tilde{I}_2| & \lesssim h^{5/2} \left(|u|_{3,\infty,\Omega} + h^{1/2} |\log h|^{1/2} |u|_{2,\infty,\Omega} \right) |v_h|_{1,\Omega} \\ & \lesssim h^{5/2} \|u\|_{3,\infty,\Omega} |v_h|_{1,\Omega}. \end{aligned}$$

Thus the final estimate for I_2 is

$$|I_2| \lesssim h^2 \|u\|_{3,\infty,\Omega} |v_h|_{1,\Omega}. \quad (3.9)$$

Combining (3.7) and (3.9), we finally obtain the interpolation estimate (3.4). \square

Theorem 3.1. *Assume that the solution of (3.1) satisfies $u \in W^{3,\infty}(\Omega)$. Further, assume the hypotheses of Lemma 3.1. Then*

$$\|u_h - u_I\|_{1,\Omega} \lesssim h^2 \|u\|_{3,\infty,\Omega}.$$

Proof. We begin with the identity

$$\begin{aligned} B(u - u_I, v_h) &= \sum_{\tau \in \mathcal{T}_h} \int_{\tau} \nabla(u - u_I) \cdot \mathcal{D}_{\tau} \nabla v_h \, dx + \sum_{\tau \in \mathcal{T}_h} \int_{\tau} \nabla(u - u_I) \cdot (\mathcal{D} - \mathcal{D}_{\tau}) \nabla v_h \, dx \\ &\quad + \int_{\Omega} (u - u_I)(\mathbf{b} \cdot \nabla v_h + c v_h) \, dx = I_1 + I_2 + I_3. \end{aligned}$$

The first term I_1 is estimated by Lemma 3.1. I_2 and I_3 can be easily estimated by

$$|I_2| + |I_3| \lesssim h^2 \|u\|_{2,\Omega} \|v_h\|_{1,\Omega}.$$

Thus

$$|B(u - u_I, v_h)| \lesssim h^2 \|u\|_{3,\infty,\Omega} \|v_h\|_{1,\Omega}.$$

Using the inf-sup condition

$$\begin{aligned} \mu \|u_h - u_I\|_{1,\Omega} &\leq \sup_{v_h \in \mathcal{V}_h} \frac{B(u_h - u_I, v_h)}{\|v_h\|_{1,\Omega}} \\ &= \sup_{v_h \in \mathcal{V}_h} \frac{B(u - u_I, v_h)}{\|v_h\|_{1,\Omega}} \lesssim h^2 \|u\|_{3,\infty,\Omega} \end{aligned}$$

completes the proof of the theorem. \square

3.3. Superconvergence between the gradient recovered by SPR and true gradient

Superconvergence Patch Recovery (SPR) is a gradient recovery method introduced by Zienkiewicz and Zhu in [6]. The SPR-recovery gradient is used to produce the ZZ error estimator in [7], namely ZZ-SPR. This method is widely used in engineering practices for its robustness in a posteriori error estimates and its efficiency in computer implementation.

We define \mathcal{N}_h as the nodal set of a Par6 tessellation \mathcal{T}_h . Given $z \in \mathcal{N}_h$, we consider an element patch ω around z and we choose z as the origin of a local coordinates. Under this coordinate system, we let (x_j, y_j, z_j) be the barycenter of a tetrahedron $\tau_j \subset \omega, j = 1, 2, \dots, m$. From further observation on Par6, we will find the following geometric condition is satisfied for any interior vertex z :

$$\frac{1}{m} \sum_{j=1}^m (x_j, y_j, z_j) = 0. \quad (3.10)$$

This geometric condition holds because of the highly symmetric structure of Par6. And for the boundary vertices, the corresponding geometric condition is:

$$\frac{1}{m} \sum_{j=1}^m (x_j, y_j, z_j) = \mathcal{O}(h^{1+\alpha})(1, 1, 1),$$

where $\alpha \in [0, 1]$. While the tetrahedrons with boundary vertices only occupy small volume compared with whole domain Ω , that is to say

$$\sum_{\tau \text{ with boundary vertices}} |\tau| \lesssim Nh^3 \lesssim h,$$

where N is the number of tetrahedrons with boundary vertices.

Let $u_l \in \mathcal{V}_h$ be the linear interpolation of a given function u . We shall discuss a gradient recovery operator G_h and prove the superconvergence property between ∇u and $G_h u_l$. The value of $G_h u_l$ is first determined at a vertex, and then linearly interpolated over the whole domain. SPR uses the local discrete least-squares fitting to seek linear functions $p_l \in P_1(\omega)$ ($l = 1, 2, 3$), such that

$$\sum_{j=1}^m [p_l(x_j, y_j, z_j) - \partial_l u_l(x_j, y_j, z_j)] q(x_j, y_j, z_j) = 0, \quad \forall q \in P_1(\omega), \quad l = 1, 2, 3. \quad (3.11)$$

Then we define $G_h u_l(z) = (p_1(0, 0, 0), p_2(0, 0, 0), p_3(0, 0, 0))$. The existence and uniqueness of the minimizer in (3.11) can be found in [24].

Lemma 3.2. *Let ω be an element patch around a vertex $z \in \mathcal{N}_h$, let $u \in W_\infty^3(\omega)$, and let $G_h u_l(z)$ be produced by the local discrete least-squares fitting under condition (3.10). Then*

$$|G_h u_l(z) - \nabla u(z)| \lesssim h^2 \|u\|_{3, \infty, \omega}.$$

Proof. Set $q = 1$ in (3.11) to obtain

$$\sum_{j=1}^m p_l(x_j, y_j, z_j) = \sum_{j=1}^m \partial_l u_l(x_j, y_j, z_j).$$

Therefore,

$$\begin{aligned} & p_l(0, 0, 0) - \frac{1}{m} \sum_{j=1}^m \partial_l u_l(x_j, y_j, z_j) \\ &= p_l(0, 0, 0) - \frac{1}{m} \sum_{j=1}^m p_l(x_j, y_j, z_j) \\ &= -\frac{1}{m} \nabla p_l(0, 0, 0) \cdot \sum_{j=1}^m (x_j, y_j, z_j) = 0, \end{aligned} \quad (3.12)$$

where Taylor expansion and condition (3.10) have been used. Next,

$$\begin{aligned} & \frac{1}{m} \sum_{j=1}^m \partial_l u_I(x_j, y_j, z_j) - \partial_l u(0, 0, 0) \\ &= \frac{1}{m} \sum_{j=1}^m \partial_l (u_I - u)(x_j, y_j, z_j) + \frac{1}{m} \sum_{j=1}^m [\partial_l u_I(x_j, y_j, z_j) - \partial_l u(0, 0, 0)] \\ &= \frac{1}{m} \sum_{j=1}^m \partial_l (u_I - u)(x_j, y_j, z_j) + \frac{1}{m} \nabla \partial_l u(0, 0, 0) \cdot \sum_{j=1}^m (x_j, y_j, z_j) + R(u), \end{aligned}$$

where, by Taylor expansion, the high order term $R(u)$ is estimated by

$$|R(u)| \lesssim h^2 \|u\|_{3, \infty, \omega}.$$

Therefore,

$$\left| \frac{1}{m} \sum_{j=1}^m \partial_l u_I(x_j, y_j, z_j) - \partial_l u(0, 0, 0) \right| \lesssim h^2 \|u\|_{3, \infty, \omega}. \quad (3.13)$$

Combining (3.12) and (3.13), we have proved

$$|p_l(0, 0, 0) - \partial_l u(0, 0, 0)| \lesssim h^2 \|u\|_{3, \infty, \omega}.$$

This completes the proof of the lemma. \square

Lemma 3.3. *The recovery operator G_h satisfies*

$$G_h v(\mathbf{z}) = \sum_{j=1}^m c_j \nabla v(x_j, y_j, z_j), \quad \sum_{j=1}^m c_j = 1,$$

unconditionally. Furthermore, $c_j > 0$ for the locate discrete least-squares fitting under the condition (3.10).

Proof. Let $p_l(x, y, z) = a_0 + a_1 x + a_2 y + a_3 z$. Then for the local discrete least-squares fitting, a_i 's are given by

$$\begin{pmatrix} m & \sum_j x_j & \sum_j y_j & \sum_j z_j \\ \sum_j x_j & \sum_j x_j^2 & \sum_j x_j y_j & \sum_j x_j z_j \\ \sum_j y_j & \sum_j x_j y_j & \sum_j y_j^2 & \sum_j y_j z_j \\ \sum_j z_j & \sum_j x_j z_j & \sum_j y_j z_j & \sum_j z_j^2 \end{pmatrix} \begin{pmatrix} a_0 \\ a_1 \\ a_2 \\ a_3 \end{pmatrix} = \begin{pmatrix} \sum_j \partial_l u_h(x_j, y_j, z_j) \\ \sum_j x_j \partial_l u_h(x_j, y_j, z_j) \\ \sum_j y_j \partial_l u_h(x_j, y_j, z_j) \\ \sum_j z_j \partial_l u_h(x_j, y_j, z_j) \end{pmatrix}. \quad (3.14)$$

Under condition (3.10),

$$\sum_j x_j = 0, \quad \sum_j y_j = 0, \quad \sum_j z_j = 0.$$

Therefore, from (3.14) we get

$$\begin{aligned} a_0 &= \frac{1}{m} \sum_j \partial_l u_h(x_j, y_j, z_j) - \frac{a_1}{m} \sum_j x_j - \frac{a_2}{m} \sum_j y_j - \frac{a_3}{m} \sum_j z_j \\ &= \sum_j c_j \partial_l u_h(x_j, y_j, z_j) \end{aligned}$$

with $c_j = 1/m > 0$. □

Remark 3.1. Under the given condition, the recovered gradient at a vertex z is a convex combination of gradient values on the element patch surrounding z . Since Par6 is uniform tessellation, SPR has the same performance as simple averaging or weighted averaging theoretically but more robust in practice.

Theorem 3.2. Let the solution of (3.1) satisfy $u \in W_\infty^3(\Omega)$, let u_h be the solution of (3.2), and let G_h be a recovery operator defined by the local discrete least-squares fitting. Assume the tessellation is Par6 \mathcal{T}_h . Then

$$\|\nabla u - G_h u_h\|_{0,\Omega} \lesssim h^2 \|u\|_{3,\infty,\Omega}. \quad (3.15)$$

Proof. We decompose

$$\nabla u - G_h u_h = (\nabla u - (\nabla u)_I) + ((\nabla u)_I - G_h u_I) + G_h(u_I - u_h), \quad (3.16)$$

where $(\nabla u)_I \in \mathcal{V}_h^3$ is the linear interpolation of ∇u . By the standard approximation theory,

$$\|\nabla u - (\nabla u)_I\|_{0,\Omega} \lesssim h^2 |u|_{3,\Omega}. \quad (3.17)$$

Using Lemma 3.2, we have

$$\begin{aligned} \|(\nabla u)_I - G_h u_I\|_{0,\Omega} &\leq \left(\sum_{\tau \in \mathcal{T}_h} |\tau| \sum_{z \in \mathcal{N}_h \cap \bar{\tau}} |G_h u_I(z) - \nabla u(z)|^2 \right)^{1/2} \\ &\lesssim h^2 \|u\|_{3,\infty,\Omega} |\Omega|^{1/2} \lesssim h^2 \|u\|_{3,\infty,\Omega}. \end{aligned} \quad (3.18)$$

Similarly, by the fact proved in Lemma 3.3, that $G_h v(z)$ is a convex combination of $\nabla v|_\tau$ in the patch ω ,

$$\begin{aligned} \|G_h(u_I - u_h)\|_{0,\Omega} &\leq \left(\sum_{\tau \in \mathcal{T}_h} |\tau| \sum_{z \in \mathcal{N}_h \cap \bar{\tau}} |G_h(u_I - u_h)(z)|^2 \right)^{1/2} \\ &\lesssim \left(\sum_{\tau \in \mathcal{T}_h} |\tau| |\nabla(u_I - u_h)|_\tau^2 \right)^{1/2} \\ &= \|\nabla(u_I - u_h)\|_{0,\Omega} \lesssim h^2 \|u\|_{3,\infty,\Omega}, \end{aligned} \quad (3.19)$$

where Theorem 3.1 has been used. Combining (3.16)-(3.19), we obtain the final estimation (3.15). □

4. Numerical substantiation

In this section, we present a simple numerical example to verify the theoretical results deduced in previous section. The superconvergence order of $\|\nabla u - G_h u_h\|_{0,\Omega}$ for linear finite element solution on Par6 tessellation is close to 2, coinciding with the theoretical results exactly.

The linear finite element solution of the following Poisson equation is considered

$$\begin{aligned} -\Delta u &= f && \text{in } \Omega, \\ u &= g && \text{on } \partial\Omega, \end{aligned} \tag{4.1}$$

where Ω is a 3D-bounded Lipschitz domain with boundary $\partial\Omega$, f and g are smooth, and the solution u of equation (4.1) is assumed to be sufficiently smooth. The right hand side f is chosen to be $3\sin(x + y + z)$, thus the exact solution is $u = \sin(x + y + z)$ and the boundary condition is properly imposed.

The experiment is conducted on Par6 tessellation, for which the whole parallelepiped domain Ω is divided into small parallelepiped and then each small parallelepiped is subdivided into six identical tetrahedrons (see Fig. 1). The SPR method is performed on a sequence of meshes with the sizes being $h = 0.100, 0.050, 0.033, 0.025$. The error estimation and convergence order are shown in Table 2 and Fig. 5.

Table 2: Error estimation and convergence order of the recovered gradient on Par6.

Mesh size h	SPR $\ \nabla u - G_h u_h\ _{0,\Omega}$
0.100	2.02e-3
0.050	5.18e-4
0.033	2.32e-4
0.025	1.32e-4
Order	1.9779

The convergence order corresponds to the absolute value of slope in the figure, which is approximately 2, coinciding with our theoretical results exactly.

5. Conclusions and future works

In this paper, a theoretical analysis of linear finite elements superconvergence on Par6 tessellation is presented. Involving the post-processing gradient recovery method SPR, we show that the recovered gradient $G_h u_h$ is a superconvergent approximation to ∇u in a order of 2. Par6 pattern is a particular CVT structure which can be considered optimal in three dimension [19]. Thus, our theoretical analysis bears significance to the Centroidal Voronoi tessellation based finite element superconvergence.

In future, the theoretical extension of superconvergence property on general CVT meshes will be explored both for two- and three-dimensions. The low order terms in

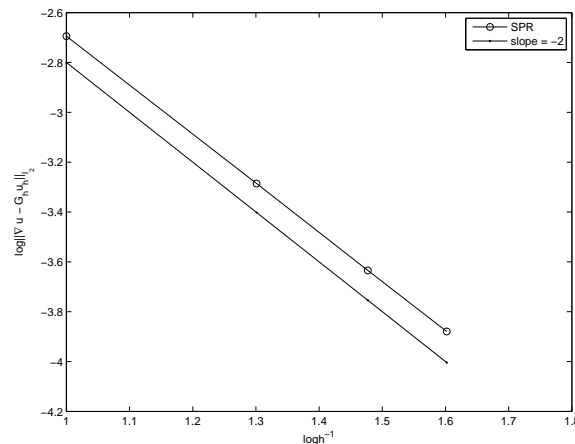


Figure 5: Error estimation and convergence rate of the recovered gradient on Par6.

the asymptotic expansion of the local error are totally canceled because of the highly symmetric structure of Par6. The general CVT meshes also enjoy some degree of symmetry and can be considered as quasi-uniform meshes. Consequently, to analyze the superconvergence property on general CVT meshes, the key is to deduce some symmetric geometry condition from the CVT mesh generation procedure.

Acknowledgments This work is partially supported by Singapore AcRF RG59/08 (M52110092) and Singapore NRF 2007 IDM-IDM002-010.

References

- [1] L. B. WAHLBIN, *Superconvergence in Galerkin Finite Element Methods*, Lecture Notes in Mathematics vol. 1605. Springer: Berlin, 1995.
- [2] M. KRÍŽEK, *Superconvergence phenomena in the finite element method*, Computer Methods in Applied Mechanics and Engineering, 116 (1994), pp. 157–163.
- [3] C. CHEN AND Y. HUANG, *High Accuracy Theory of Finite Element Methods*, Hunan Science Press: Hunan, China, 1995 (in Chinese).
- [4] O. C. ZIENKIEWICZ AND J. ZHU, *A simple error estimator and adaptive procedure for practical engineering analysis*, International Journal for Numerical Methods in Engineering, 24 (1987), pp. 337–357.
- [5] Z. ZHANG AND A. NAGA, *A new finite element gradient recovery method: superconvergence property*, SIAM Journal on Scientific Computing, 26 (2005), pp. 1192–1213.
- [6] O. C. ZIENKIEWICZ AND J. ZHU, *The superconvergence patch recovery and a posteriori error estimates, part I: the recovery technique*, International Journal for Numerical Methods in Engineering, 33 (1992), pp. 1331–1364.
- [7] O. C. ZIENKIEWICZ AND J. ZHU, *The superconvergence patch recovery and a posteriori error estimates, part II: error estimates and adaptivity*, International Journal for Numerical Methods in Engineering, 33 (1992), pp. 1365–1382.
- [8] H. WU AND Z. ZHANG, *Can We Have Superconvergence Gradient Recovery Under Adaptive Meshes?*, SIAM Journal of Numerical Analysis 45 (2007), pp. 1701–1722.

- [9] Q. DU AND L. JU, *Numerical simulations of the quantized vortices in a thin superconducting hollow sphere*, J. Comput. Phys., 201 (2004), pp. 511-530.
- [10] Q. DU AND L. JU, *Finite volume methods on spheres and spherical centroidal Voronoi meshes*, SIAM J. Numer. Anal., 43 (2005), pp. 1673-1692.
- [11] R. E. BANK AND J. XU, *Asymptotically exact a posteriori error estimators, Part I: Grid with superconvergence*, SIAM Journal of Numerical Analysis, 41 (2003), pp. 2294-2312.
- [12] R. E. BANK AND J. XU, *Asymptotically exact a posteriori error estimators, Part II: General Unstructured Grids*, SIAM Journal of Numerical Analysis, 41 (2003), pp. 2313-2332.
- [13] Y. HUANG, H. QIN AND D. WANG, *Centroidal Voronoi tessellation-based finite element superconvergence*, International Journal for Numerical Methods in Engineering, 76 (2008), pp. 1819-1839.
- [14] Y. HUANG, H. QIN, D. WANG AND Q. DU, *Convergent adaptive finite element method based on Centroidal Voronoi Tessellation and superconvergence*, preprint.
- [15] J. CHEN, Y. HUANG AND D. WANG, *Three Dimensional Superconvergent Gradient Recovery On tetrahedral meshes*, preprint.
- [16] J. BRANDTS AND M. KŘÍŽEK, *Gradient superconvergence on uniform simplicial partition of polytopes*, IMA Journal of Numerical Analysis, 23 (2003), pp. 489-505.
- [17] L. CHEN, *Superconvergence of tetrahedral linear finite elements*, International Journal of Numerical Analysis and Modeling, 3 (2004), pp. 273-282.
- [18] D. J. NAYLOR, *Filling space with tetrahedra*, International Journal for Numerical Methods in Engineering, 44 (1999), pp. 1383-1395.
- [19] Q. DU AND D. WANG, *The optimal centroidal Voronoi tessellations and the Gersho's conjecture in the three-dimensional space*, Computers and Mathematics with Applications, 49 (2005), pp. 1355-1373.
- [20] A. GERSHO, *Asymptotically optimal block quantization*, IEEE Transactions on Information Theory, 25 (1979), pp. 373-380.
- [21] D. NEWMAN, *The Hexagon theorem*, IEEE Transactions on Information Theory, 28 (1982), pp. 137-139.
- [22] R. M. GRAY AND D. L. NEUHOFF, *Quantization*, IEEE Transactions on Information Theory, 44 (1998), pp. 2325-2383.
- [23] E. S. BARNES AND N. J. A. SLOANE, *The optimal lattice quantizer in three dimensions*, SIAM Journal on Algebraic and Discrete Methods, 4 (1983), pp. 30-41.
- [24] B. LI AND Z. ZHANG, *Analysis of a class of superconvergence patch recovery techniques for linear and bilinear finite elements*, Numerical Methods for Partial Differential Equations, 15 (1999), pp. 151-167.